On the effects of trigonometric and exponential terms on the best theory diagrams for metallic, multilayered, and functionally graded plates

(Article begins on next page)

03 February 2023

On the Effects of Trigonometric and Exponential Terms on the Best Theory Diagrams for Metallic and Multilayered Plates

J.L. Mantari[a1], J Yarasca[a], M. Petrolo[b], E. Carrera[b]

[a] Faculty of Mechanical Engineering, Universidad de Ingeniería y Tecnología (UTEC), Medrano Silva 165, Barranco, Lima, Peru

[b] Department of Mechanical and Aerospace Engineering, Politecnico di Torino, Corso Duca degli Abruzzi 24, 10129 Torino, Italy

Abstract

This paper presents Best Theory Diagrams (BTDs) employing combinations of Maclaurin, trigonometric and exponential terms to build two-dimensional theories for metallic and multilayered plates. The BTD is a curve in which the least number of unknown variables to meet a given accuracy requirement is read. The present refined models are Equivalent Single Layer (ESL) and are implemented by using the Unified Formulation developed by Carrera (CUF). The theories that belong to the BTD are obtained using the Axiomatic/Asymptotic method and genetic algorithms. Closed-form, Navier-type solutions have been obtained in the case of simply supported plates loaded by a bisinuisoidal transverse pressure. The influence of trigonometric and exponential terms in the BTDs has been studied for different materials and length-to-thickness ratios. The results show that the addition of such terms can lead to enhanced BTDs in which fewer unknown variables than pure Maclaurin expansions are needed to detect 3D like accuracies.

Keywords: Plates, CUF, Best Theory Diagram, Multilayer.

---

[1]Corresponding Author email: jmantari@utec.edu.pe Tel: +00511 3540070; Cell: +0051 96224551;

1. Introduction

Metallic and multilayered plates are extensively used in various engineering applications. With the high demand for such structures, efficient and reliable analysis methods are required. Over the last decades, several relevant contributions have been

made to improve the classical plate theories (CPT) originally developed for thin isotropic plates [1-3]. In fact, the CPT accuracy is poor when the plate is considerably thick; local effects are present or in the case of transverse anisotropy and high deformability. First shear deformation theories (FSDT) alleviate these problems [4-7]. Nevertheless, none of these theories provides accurate transverse stress distributions. More accurate theories exploit various strategies; such as higher order shear deformation theories (HSDT) that assume quadratic, cubic, higher order and non-polynomial terms to improve the displacement field along the thickness direction [8-21]; the use of the Zig-Zag approach [22, 23]; the adoption of mixed variational tools [24]. The implementation of refined models can be carried out using Equivalent Single Layer (ESL) or Layer-Wise approaches. Excellent reviews of existing ESL and LW models can be found in [25-29].

The structural models mentioned above can be defined as axiomatic. In fact, they are based on the intuition of scientists to create simplified kinematic models, which neglect some characteristics of the mechanical behavior of a structure. Another approach is the asymptotic method in which the expansion of characteristic parameters of the structures (e.g., the length-to-thickness ratio) is used to build an asymptotic series. Those terms that exhibit the same order of magnitude as the parameter when it vanishes are retained. Excellent contributions to the asymptotic method can be found here [30, 31].

The present work is embedded in the framework of the Carrera Unified Formulation (CUF). According to CUF, the governing equations are given regarding the so-called fundamental nuclei whose form does not depend on either the expansion order nor on the choices made for the base functions. More details on CUF can be found in [32, 33]. ESL and LW models were successfully developed in CUF, as reported in [34]. Refined theories lead to accurate analysis at the expense of higher computational cost. To develop accurate plate theories with lower computational effort, Carrera and Petrolo [35, 36] presented the Axiomatic/Asymptotic Method (AAM). This method is based on a preliminary axiomatic choice of a refined model obtained through CUF and evaluates the effectiveness of each higher order term of a structural theory against a reference solution. Those variables whose influence cannot be neglected are retained. The AAM has been applied to several problems, including: static and free vibration of beams [35, 37], metallic and composite plates [36, 38], shells [39, 40], LW models [41, 42], advanced models based on the Reissner Mixed Variational Theorem [43], and piezoelectric plates [44].

The use of AAM led to the introduction of the BTD [45, 46]. The BTD is a curve in which the minimum number of expansion terms – i.e. unknown variables - required to meet a given accuracy can be read; or, conversely, the best accuracy provided by a given amount of variables can be read. In [47], BTDs were presented for ESL and LW composite plate models based on Maclaurin and Legendre polynomial expansions of the unknown variables along the thickness.

The present work presents BTDs using Maclaurin, trigonometric and exponential thickness expansions. Some models with trigonometric thickness functions have been developed in the literature. Shimpi and Ghugal [13, 48] proposed LW trigonometric shear deformation theories for the analysis of composite beams. A zig-zag model was developed by Arya et al. [14] using a sine term to represent the non-linear displacement field across the thickness in symmetrically laminated beams. Other contributions made use of meshless methods [15-17]. Hybrid Maclaurin-trigonometric models were proposed by Mantari et al. [49, 50] for bending, free vibration and buckling analysis of laminated beams. Mantari et al. [51] presented a generalized hybrid formulation for the study of functionally graded sandwich beams, which was extended to the Finite Element method by Yarasca et al. [52]. Most recent developments have dealt with thermal problems [53] and FGM plates [54]. The trigonometric and exponential functions employed in this paper were selected according to Filippi et al. [55, 56]. Due to the high expansion order employed, the BTDs are obtained using a genetic algorithm. The application of this method to develop accurate reduced models with lower computational effort was presented on [46].

The present paper is organized as follows: a description of the adopted formulation is provided in Section 2; the AAM is presented in Section 3; the BTD is introduced in Section 4; the results are commented in Section 5, and the conclusions are presented in Section 6.

2. Carrera Unified Formulation for Plates

Plate geometry and notations are given in Fig 1. According to CUF [34], the displacement of a plate model can be described as

$$\boldsymbol{u} = F_\tau \cdot \boldsymbol{u}_\tau \qquad \tau = 1, 2, \dots, N+1 \tag{1}$$

where $\boldsymbol{u}$ is the displacement vector (u_x, u_y, u_z) whose components are the displacements along the x, y, z reference axes. F_τ are the expansion functions and $\boldsymbol{u}_\tau$ $(u_{x_\tau}, u_{y_\tau}, u_{z_\tau})$ are

the displacements variables. If an ESL approach is employed, the behavior of a multilayered plate is analyzed considering it as a single equivalent lamina. In this case, F_τ functions can be Maclaurin functions of z defined as $F_\tau = z^{\tau-1}$. The ESL models are indicated as EDN, where N is the expansion order. An example of an ED4 displacement field is reported as:

$$u_x = u_{x_1} + z\,u_{x_2} + z^2 u_{x_3} + z^3 u_{x_4} + z^4 u_{x_5}$$

$$u_y = u_{y_1} + z\,u_{y_2} + z^2 u_{y_3} + z^3 u_{y_4} + z^4 u_{y_5}$$

$$u_z = u_{z_1} + z\,u_{z_2} + z^2 u_{z_3} + z^3 u_{z_4} + z^4 u_{z_5} \tag{2}$$

The present paper investigates the influence of trigonometric and exponential terms. Table 1 shows the complete, ED17 set of terms adopted; that is, 51 unknown variables were considered. The displacement field of ED17 has 15 Maclaurin terms - the ED4 terms -, 24 trigonometric terms and 12 exponential terms. For instance, the full expression of the displacement along x is

$$u_x =$$

$$u_{x_1} + z\,u_{x_2} + z^2 u_{x_3} + z^3 u_{x_4} + z^4 u_{x_5} + \sin\left(\frac{\pi z}{h}\right)u_{x_6} + \sin\left(\frac{2\pi z}{h}\right)u_{x_7} + \sin\left(\frac{3\pi z}{h}\right)u_{x_8} +$$

$$\sin\left(\frac{4\pi z}{h}\right)u_{x_9} + \cos\left(\frac{\pi z}{h}\right)u_{x_{10}} + \cos\left(\frac{2\pi z}{h}\right)u_{x_{11}} + \cos\left(\frac{3\pi z}{h}\right)u_{x_{12}} + \cos\left(\frac{4\pi z}{h}\right)u_{x_{13}} +$$

$$e^{\frac{z}{h}}u_{x_{14}} + e^{\frac{2z}{h}}u_{x_{15}} + e^{\frac{3z}{h}}u_{x_{16}} + e^{\frac{4z}{h}}u_{x_{17}} \tag{3}$$

where h is the thickness of the plate. Governing equations are herein omitted for the sake of brevity, but can be found in [36]. In this paper, the closed-form solution proposed by Navier for simply supported plates is exploited. The displacements are therefore expressed in the following harmonic form,

$$u_x = \sum_{m,n} U_x \cdot \cos\left(\frac{m\pi x}{a}\right) \sin\left(\frac{n\pi y}{b}\right)$$

$$u_y = \sum_{m,n} U_y \cdot \cos\left(\frac{m\pi x}{a}\right) \sin\left(\frac{n\pi y}{b}\right)$$

$$u_z = \sum_{m,n} U_z \cdot \cos\left(\frac{m\pi x}{a}\right) \sin\left(\frac{n\pi y}{b}\right) \tag{4}$$

where U_x, U_y and U_z are the amplitudes, m and n are the number of waves, and a and b are the dimensions of the plate in the x and y directions, respectively.

3. Axiomatic Asymptotic Method

Literature survey has shown that accurate plate analyses can be obtained by introducing higher order terms in a plate model. The introduction of higher order terms offers better accuracies at the expense of higher computational cost. The AAM can be seen as a method to analyse the contribution of each term to a given problem and retain only the effective ones to preserve the accuracy of a higher order model and minimize the computational cost. The AAM procedure can be summarized as follows [35, 36],

1. Parameters such as geometry, boundary conditions, loadings, materials and layer layouts are fixed.

2. A set of output parameters is chosen, such as displacement and stress components.

3. A theory is fixed; that is the displacement variables to be analyzed are defined.

4. A reference solution is defined; in the present work, fourth-order LW models (LD4) are adopted, since these fourth-order model offer an excellent agreement with the three-dimensional solutions [42].

5. The CUF is used to generate the governing equations for the considered theories.

6. Each variable displacement effectiveness is numerically established measuring the loss of accuracy on the chosen output parameters compared with the reference solution.

7. The most suitable kinematic model for a given structural problem is then obtained by discarding the noneffective displacement variables.

A graphical notation is introduced to represent the results. This consists of a table with three rows, and some columns equal to the number of the displacement variable used in the expansion. As an example, an ED4 model (full model) and a reduced model in which the term u_{x_2} is deactivated is shown in Table 2. The meaning of the symbols ▲ and △ is reported in Table 3. The displacement field of Table 2 is

$$u_x = u_{x_1} + \qquad z^2 u_{x_3} + z^3 u_{x_4} + z^4 u_{x_5}$$

$$u_y = u_{y_1} + z\, u_{y_2} + z^2 u_{y_3} + z^3 u_{y_4} + z^4 u_{y_5}$$

$$u_z = u_{z_1} + z\, u_{z_2} + z^2 u_{z_3} + z^3 u_{z_4} + z^4 u_{z_5} \qquad (5)$$

4. Best Theory Diagram

The construction of reduced models through the AAM can lead to a diagram in which, for a given problem, each reduced model is associated with the number of active terms and its error computed on a reference solution. This diagram allows editing an arbitrary given theory to get a lower number of terms for a given error, or to increase the accuracy while keeping the computational cost constant. Considering all the reduced models, it is possible to recognize that some of them provide the lowest error for a given number of terms. These models represent a Pareto front for this specific problem. As in [46], the Pareto front is defined as the best theory diagram (BTD). This curve is case dependent since it changes for several problems, i.e. different materials, geometries, boundary conditions and output parameters.

The computational cost required for the BTD construction can be considerable. The number of all possible combinations of active/not-active terms for a given model is equal to 2^M, where M is the number of unknown variables (DOF) of the model. In the case considered in this paper, M is equal to 51. As demonstrated in [46], a genetic algorithm can be used to build BTDs with reduced computational costs. In genetic algorithms, a solution vector $\boldsymbol{x} \in \boldsymbol{X}$, where $\boldsymbol{X}$ is the solution space, is called an individual or a *chromosome*. Chromosomes are made of discrete units called *genes*. Each gene controls one or more features of the individual. Genetic algorithms operate with a collection of chromosomes, called a *population*. The population is normally randomly initialized. As the search evolves, the population includes fitter and fitter solutions, and eventually it converges, meaning that it is dominated by a single solution. Genetic algorithms use two operators to generate new solutions from existing ones: *crossover* and *mutation*. In the crossover, generally two chromosomes, called *parents*, are combined together to form new chromosomes, called *offsprings*. The parents are selected among existing ones base on their fitness. The mutation operator introduces random changes at gene level. Each chromosome has a fitness value based on its rank in the population. The population is ranked according to the dominance rule. The fitness of each chromosome is evaluated throught the following formula:

$$r_i(\boldsymbol{x_i}, t) = 1 + nq(\boldsymbol{x_i}, t) \tag{6}$$

where $nq(\boldsymbol{x}, t)$ is the number of solutions dominating $\boldsymbol{x}$ at generation t. A lower rank corresponds to a better solution. The number of offsprings the parents have are

determined by their rank in the population. A complete explanation of genetic algorithms can be found in [57].

Each plate theory has been considered as an individual. The genes are the terms of the expansion along the thickness of the three displacement fields in this manner. Each gene can be active or not, the deactivation of a term is obtained by exploiting a penalty or row- column elimination technique. The graphical notation is shown in Fig 2. Each individual is therefore described by the number of active terms and its error that is computed on a reference solution. The dominance rule is applied through these two parameters to evaluate the individual fitness. The error of the new models on a reference solution was evaluated through the following formula:

$$e = 100 \frac{\sum_{i=1}^{N_p} |Q^i - Q^i_{ref}|}{max Q_{ref} \cdot N_p} \tag{7}$$

where Q can be a stress/displacement component ($\bar{\sigma}_{xx}$ in this article) and N_p is the number of points along the thickness on which the entity Q is computed. Each chromosome of the new population its ranked and new dominant chromosomes are selected. More details about the implementation of genetic algorithms for BTD can be found in [46]. In this paper, 30 generations were used and the initial population was set to 1200.

5. Results and discussion

Results deal with simply supported square plates. The load is bisinusoidal and equal to:

$$p = \bar{p}_z \cdot sin\left(\frac{m\pi x}{a}\right) sin\left(\frac{n\pi y}{b}\right), \tag{8}$$

with $a = b = 0.1\ m$. $\bar{p}_z$ is the applied load amplitude, $\bar{p}_z = 1\ kPa$, and m and n are equal to 1. All the reduced models are developed for σ_{xx}, which is computed at $\left[a/2, b/2, z\right]$, with $-\frac{h}{2} \leq z \leq \frac{h}{2}$, where h is the total thickness of the plate. The stress σ_{xx} is normalized according to:

$$\bar{\sigma}_{xx} = \frac{\sigma_{xx}}{\bar{p}_z \cdot (a/h)^2} \tag{9}$$

The numerical investigation has considered two metallic plates: a single plate made of aluminium and a two-layer plate of aluminium and titanium.

5.1. Aluminum plate

The material properties are E= 73 GPa and $v = 0.34$. The length-to-thickness ratios are equal to 2.5, 5 and 50.

An LD4 model assessment was carried out. The results are reported in Table 4; the three-dimensional exact elasticity results are obtained as in [58]. The results offered by the LD4 model are in excellent agreement with the reference solution. Consequently, the LD4 model is used for the computation of the reference solution in this paper.

The first method that was used to build the BTD is based on the evaluation of all possible combinations of an ED4 polynomial model obtain by the AAM. Figure 3 shows the error of each theory and the corresponding BTD. Figure 4 shows the difference between the BTDs built from a polynomial, ED4 model and the model with trigonometric and exponential terms. The former is indicated as *Pol,* and the corresponding BTD was obtained using the AAM only. The latter is referred to as *Hybrid,* and the related BTD was obtained using the genetic algorithm. For the sake of clarity, the entire BTD for the hybrid model was not reported. In fact, only the last 15 terms portion of the curve is shown to have a direct comparison with the ED4 model. Table 5 presents the best hybrid models for $a/h = 2.5$; M_E indicates the number of active terms. For instance, the best hybrid model for $\bar{\sigma}_{xx}$ with five unknown variables is the following:

$$u_x = zu_{x_2}$$

$$u_y = z^3 u_{y_4} + \sin\left(\frac{3\pi z}{h}\right) u_{y_8} \qquad (10)$$

$$u_z = u_{z_1} + e^{\frac{4z}{h}} u_{z_{17}}$$

Likewise, the best model for $\bar{\sigma}_{xx}$ obtained via ED4 with five unknown variables is:

$$u_x = u_{x_1} + zu_{x_2}$$

$$u_y = z^3 u_{y_4} \qquad (11)$$

$$u_z = u_{z_1} + zu_{z_2}$$

Table 6 shows the comparison between the best models obtained via ED4 and those from the hybrid model. The plate model of Eq. (10) can detect the in-plane stress with 1.0681 % of error on the layer-wise solution, while in comparison the plate model of

Eq. (11) has an error of 3.0488 %. Tables 7 and 8 show the best models for $a/h = 5$. The $\bar{\sigma}_{xx}$ distribution along the thickness is reported for different plate length-to-thickness ratios in Fig. 5. The evaluation of $\bar{\sigma}_{xx}$ is performed by means of the reduced models reported in Tables 5 and 7. The notation used is NHRM, where N is the number of variables in the hybrid reduced models (HRM).

The results herein reported for the aluminium plate suggest that:

- A genetic algorithm makes it possible to construct BTDs for higher-order hybrid theories when the AAM is not viable.

- BTDs for thick plates are enhanced by trigonometric and exponential terms. In fact, these terms lower the error for a given number of variables on Maclaurin-based BTDs.

- More often than not, the exponential terms are more important than the trigonometric ones.

- On the other hand, less significant improvements were observed in the case of thin plates. That is, the influence of trigonometric and exponential terms is less relevant.

- In general, the adoption of reduced models enhances the computational efficiency to a great extent. In fact, very few displacement variables are needed to meet accuracy levels higher than 95 %.

5.2. Bimetallic plate

A two-layer plate made of two isotropic layers has been considered. Aluminium and titanium were used. The former has E= 70.3 GPa and $v = 0.33$. The latter has E= 110 GPa and $v = 0.34$. The length-to-thickness ratios are equal to 2.5 and 5. Each layer has the same thickness in both cases.

The BTD for $a/h = 2.5$ and $a/h = 5$ length-to-thickness ratios are reported in Fig. 6. The best models for $a/h = 2.5$ are given in Table 9, whereas Table 10 shows the comparison between the best hybrid and Maclaurin models. Figure 7 shows the stress distribution via various best models. Tables 11 and 12 present the best models for $a/h = 5$. For intance, the best hybrid model with six degrees of freedom for the $a/h = 2.5$ case is the following:

$$u_x = zu_{x_2}$$

$$u_y = u_{y_1} + \cos\left(\frac{2\pi z}{h}\right)u_{y_{11}} + e^{\frac{z}{h}}u_{y_{14}} \qquad (12)$$

$$u_z = u_{z_1} + \cos\left(\frac{\pi z}{h}\right)u_{z_{10}}$$

Likewise, the best Maclaurin model for $\bar{\sigma}_{xx}$ with six degrees of freedom for the $a/h = 2.5$ case is:

$$u_x = zu_{x_2} + z^3 u_{y_4}$$

$$u_y = u_{y_1} + zu_{y_2} + z^2 u_{y_3} \qquad (13)$$

$$u_z = u_{z_1}$$

The results reported for the bimetallic plate suggest that:

- As for the one-layer case, higher the thickness, more important are the trigonometric and exponential terms.
- In particular, the trigonometric terms are more effective than the exponential terms for the bimetallic composite plate studied.

6. Conclusions

Best Theory Diagrams for metallic and multilayered plates have been presented in this paper. BTDs are curves in which, for a given problem, the minimum number of unknown variables necessary to meet an accuracy requirement can be read; or, for a given number of variables, the minimum error that can be obtained is provided. The axiomatic/asymptotic method and genetic algorithms have been employed together with the Carrera Unified Formulation to develop refined ESL models. In particular, a combination of Maclaurin, trigonometric and exponential polynomials has been used to define the displacement field along the thickness of the plate. Simply-supported plates have been analyzed via Navier-type closed form solutions. The results suggest the following guidelines and recommendations:

1. In general, the use of the AAM and the BTD lead to reduced refined models with very few unknown variables, but 3D-like accuracies.
2. For thick plates, the best models built via hybrid models are more accurate than those obtained via only Maclaurin expansions.

3. For thick plates, exponential and trigonometric terms improve the accuracy of the model while maintaining a low computational cost. As the length-to-thickness increases, the effectiveness of non-polynomial terms vanishes.

4. The exponential terms are more influential to analyze thick, one-layer plates.

5. The trigonometric terms are more important for multilayer, thick plates.

The systematic computation of BTDs via AAM and CUF can represent a powerful tool to evaluate the effectiveness of any structural model. In fact, any type and order of expansions of the unknown variables can be dealt with in a unified manner. The use of genetic algorithms reduces the computational costs to a great extent. Future works should tackle the construction of BTDs for multiple outputs (stresses and displacements) and LW models.

References

[1] Cauchy AL. Sure l'equilibre et le movement d'une plaque solide. Excercies Matematique 1828;3:328-55.

[2] Poisson SD. Memoire sur l'equilibre et le mouvement des corps elastique. Mem l'Acad Sci 1829;8:357.

[3] Kirchhoff G. Über das Gleichgewicht und die Bewegung einer elastishen Scheibe. J Angew Math 1850; 40: 51-88.

[4] Reddy JN. Mechanics of laminated composite plates, theory and analysis. 2nd ed. Boca Raton, London, New York, Washington, DC: CRC Press; 2004.

[5] Reissner E. The effect of transverse shear deformation on the bending of elastic plates. J Appl Mech 1945; 12:69-76.

[6] Mindlin RD. Influence of rotatory inertia and shear in flexural motion of isotropic elastic plates. J Appl Mech 1951; 18: 1031-6.

[7] Kärger L, Wetzel A, Rolfes R, Rohwer K. A three-layered sandwich element with improved transverse shear stiffness and stress based on FSDT. Comp Struct 2006; 84: 843-54.

[8] Kant T, Owen DRJ, Zienkiewicz OC. Refined higher order C^0 plate bending element. Comput Struct 1982;15:177–83.

[9] Kant T, Kommineni JR. Large amplitude free vibration analysis of cross-ply composite and sandwich laminates with a refined theory and C^0 finite elements. Comput Struct 1989;50:123–34.

[10] Reddy JN. Mechanics of laminated composite plates and shells, theory and analysis. CRC Press; 1997.

[11] Palazotto AN, Dennis ST. Nonlinear analysis of shell structures. AIAA Series; 1992.

[12] M. Touratier. An efficient standard plate theory. International Journal of Engineering Science 1991, 29(8):901 – 916.

[13] Shimpi RP, Ghugal YM. A new layerwise trigonometric shear deformation theory for two-layered cross-ply beams. Compos Sci Technol 2001;61 (9):1271–83.

[14] Arya H, Shimpi RP, Naik NK. A zigzag model for laminated composite beams. Compos Struct 2002;56(1):21–4.

[15] Ferreira AJM, Roque CMC, Jorge RMN. Analysis of composite plates by trigonometric shear deformation theory and multiquadrics. Comput Struct 2005;83(27):2225–37.

[16] Roque CMC, Ferreira AJM, Jorge RMN. Modelling of composite and sandwich plates by a trigonometric layerwise deformation theory and radial basis functions. Compos Part B: Eng 2005;36(8):559–72.

[17] Ferreira AJM, Carrera E, Cinefra M, Roque CMC, Polit O. Analysis of laminated shells by a sinusoidal shear deformation theory and radial basis functions collocation, accounting for through-the-thickness deformations. Compos Part B: Eng 2011;42(5):1276–84.

[18] J.L. Mantari, A.S. Oktem, C. Guedes Soares: Bending response of functionally graded plates by using a new higher order shear deformation theory. Compos. Struct. 2012; 94; pp. 714-723.

[19] J.L. Mantari, C. Guedes Soares: A novel higher-order shear deformation theory with stretching effect for functionally graded plates. Compos. Struct. 2012; 94; pp. 1991-2000.

[20] J.L. Mantari, C. Guedes Soares: Generalized hybrid quasi-3D shear deformation theory for the static analysis of advanced composite plates. Compos. Struct. 94 (2012) 2561-2575. Compos. Struct. 2012; 94; pp. 2561-2575.

[21] J.L. Mantari, C. Guedes Soares: Finite element formulation of a generalized higher order shear deformation theory for advanced composite plates. Compos. Struct. 2013; 96; pp. 545-553.

[22] G.S. Lekhnitskii, Anisotropic Plates, 2nd Edition, SW Tsai and Cheron, Bordon and Breach, Cooper Station, NY, 1968.

[23] E. Carrera, Historical review of zig-zag theories for multilayered plates and shells, Appl. Mech. Rev. 2003, vol. 56, no. 3, pp. 287–308.

[24] E. Reissner, On a mixed variational theorem and on a shear deformable plate theory, Int. J.Numer.Methods Eng. 1986, vol. 23, pp. 193–198.

[25] Librescu L, Reddy JN. A critical review and generalization of transverse shear deformable anisotropic plates. In: Euromech Colloquium 219, Kassel, Refined Dynamical Theories of Beams, Plates and Shells and Their Application, I. Elishakoff and H. Irretier, Ess., Springer-Verlag, Berlin, 1986.

[26] Noor AK, and Burton WS. Assessments of Shear Deformation Theories for Multilayered Composite Plates. Applied Mechanics Reviews. 42, 1989, pp. 1-18.

[27] Noor AK, Burton WS and Bert CW. Computational Model for Sandwich Panels and Shells. Applied Mechanics Reviews. 49, 1996, pp. 155-199.

[28] Kapania K, Raciti S. Recent advances in analysis of laminated beams and plates. Part 1: Shear effects and buckling. AIAA J 1989; 27(7); 923-35.

[29] Reddy JN, Robbins DH. Theories and Computational Models for Composite Laminates. Applied Mechanics Reviews. 47, 1994, pp. 147-165.

[30] Cicala P. Systematic Approximation Approach to Linear Shell Theory, Levrotto e Bella, Torino, 1965.

[31] Berdichevsky VL. Variational-asymptotic method of shell theory construction, Prikladnaya Mat. Mek., vol. 43, pp. 664–667, 1979.

[32] Carrera E, Brischetto S, Nali P. Plates and shells for smart structures classical and advanced theories for modeling and analysis. Wiley; 2011.

[33] Carrera E, Cinefra M, Petrolo M, Zappino E. Finite element analysis of structures through unified formulation, Wiley; 2014.

[34] Carrera E. Theories and finite elements for multilayered plates and shells: a unified compact formulation with numerical assessment and benchmarking. Arch Comput Meth Eng 2003; 10(3): 215-96.

[35] Carrera E, Petrolo M. On the effectiveness of higher-order terms in refined beam theories. Journal of Applied Mechanics 2011; 78. doi: 10.1115/1.4002207.

[36] Carrera E, Petrolo M. Guidelines and recommendation to construct theories for metallic and composite plates. AIAA J. 2012; 48(12): 2852-2866.

[37] Carrera E, Miglioretti F, Petrolo M. Computations and evaluations of higher-order theories for free vibration analysis of beams. Journal of Sound and Vibration 2012; 331:4269-4284. doi: 10.1016/j.jsv.2012.04.017.

[38] Mashat DS, Carrera E, Zenkour AM, Khateeb Al. Axiomatic/asymptotic evaluation of multilayered plate theories by using single and multi-points error criteria. Compos Struct 2013; 106, pp. 393-406.

[39] Mashat DS, Carrera E, Zenkour AM, Khateeb Al. Use of axiomatic/asymptotic approach to evaluate various refined theories for sandwich shells. Compos Struct 2013; 109, pp. 139-149.

[40] Mashat DS, Carrera E, Zenkour AM, Al Katheeb SA, Lamberti A. Evaluation of refined theories for multilayered shells via Axiomatic/Asymptotic method. Journal of Mechanical Science and Technology 2014; 28(11):4663-4672

[41] Carrera E, Cinefra M, Lamberti A, Petrolo M. Results on best theories for metallic and laminated shells including Layer-Wise models. Composite Structures 2015; 126:285-298

[42] Petrolo M, Lamberti A. Axiomatic/asymptotic analysis of refined layer-wise theories for composite and sandwich plates. Mech Adv Mater Struct 2016; 23(1): 28-42.

[43] Petrolo M, Cinefra M, Lamberti A, Carrera E. Evaluation of Mixed Theories for Laminated Plates through the Axiomatic/Asymptotic Method. Composites Part B 2015; 76:260-272

[44] Cinefra M, Lamberti A, Zenkour Ashraf M, Carrera E. Axiomatic/Asymptotic Technique Applied to Refined Theories for Piezoelectric Plates. Mechanics of Advanced Materials and Structures 2015; 22(1-2):107-124

[45] Carrera E, Miglioretti F, Petrolo M. Guidelines and recommendations on the use of higher order finite elements for bending analysis of plates, Int J Comput Methods Eng Sci Mech 2011; 12(6), pp. 303-324.

[46] Carrera E, Miglioretti F. Selection of appropriate multilayered plate theories by using a genetic like algorithm. Composite Structures 2012; 94(3):1175-1186. doi: 10.1016/j.compstruct.2011.10.013.

[47] Petrolo M, Lamberti A, Miglioretti F. Best theory diagram for metallic and laminated composie plates. Mech Adv Mater Struct 2016; 23:9, pp. 1114-1130.

[48] Shimpi RP, Ghugal YM. A layerwise trigonometric shear deformation theory for two layered cross-ply laminated beams. J Reinforced Plast Compos 1999; 18, pp. 1516-1542.

[49] Mantari JL, Canales FG. A unified quasi-3D HSDT for the bending analysis of laminated beams. Aerospace Science and Technology 2016; 54, pp. 267-275.

[50] Mantari JL, Canales FG. Free vibration and buckling of laminated beams via hybrid Ritz solution for various penalized boundary conditions. Composite Structures 2016; http://dx.doi.org/10.1016/j.compstruct.2016.05.037.

[51] Mantari JL, Yarasca J. A simple and accurate generalized shear deformation theory for beams. Composite Structures 2015; 134, pp. 593-601.

[52] Yarasca J, Mantari JL, Arciniega RA. Hermite–Lagrangian finite element formulation to study functionally graded sandwich beams. Composite Structures 2016; 140, pp 567-581.

[53] Ramos IA, Mantari JL, Pagani A, Carrera E. Refined theories based on non-polynomial kinematics for the thermoelastic analysis of functionally graded plates, Journal of Thermal Stresses 2016; 39(7):835-853.

[54] Mantari JL, Ramos IA, Carrera E, Petrolo M. Static analysis of functionally graded plates using new non-polynomial displacement fields via Carrera Unified Formulation, Composites Part B 2016; 89:127-142

[55] Filippi M, Carrera E, Zenkour AM. Static analyses of FGM beams by various theories and finite elements. Composites Part B: Engineering 2015; 72, pp. 1-9.

[56] Filippi M, Petrolo M, Valvano S, Carrera E. Analysis of laminated composites and sandwich structures by trigonometric, exponential and miscellaneous polynomials and a MITC9 plate element. Composite Structures 2016; 150, pp. 103-114.

[57] Abdullah Konak, David W Coit, Alice E Smith. Multi-objective optimization using genetic algorithms: A tutorial. Reliability Engineering & System Safety 2006; 91 (9), pp. 992-1007.

[58] Carrera E, Giunta G, Brischetto S. Hierarchical closed form solutions for plates bent by localized transverse loadings. J. Zhejiang Univ. Sci. B 2007; 8 (7), pp. 1026–1037.

Tables caption

Table 1: Expansion terms of the proposed theories.

Table 2: Example of model representation.

Table 3: Symbols to indicate the status of a displacement variable.

Table 4: LD4 model assessment for an aluminium plate, $\bar{\sigma}_{xx}$

Table 5: Best hybrid models for the aluminium plate, $a/h = 2.5$.

Table 6: Comparison of the accuracy of the best ED4 and hybrid models for the aluminium plate, $a/h = 2.5$.

Table 7: Best hybrid models for the aluminium plate, $a/h = 5$.

Table 8: Comparison of the accuracy of the best ED4 and hybrid models for the aluminium plate, $a/h = 5$.

Table 9: Best hybrid models for the bimetallic plate, $a/h = 2.5$.

Table 10: Comparison of the accuracy of the best ED4 and hybrid models for the bimetallic plate, $a/h = 2.5$.

Table 11: Best hybrid models for the bimetallic plate, $a/h = 5$.

Table 12: Comparison of the accuracy of the best ED4 and hybrid models for the bimetallic plate, $a/h = 5$.

Figures caption

Figure 1. Plate reference system.

Figure 2. Displacement field of a refined model and genes of a chromosome.

Figure 3. BTD based on ED4, aluminium plate, $a/h = 2.5$.

Figure 4. BTDs based on ED4 models and built via the AAM (AAM − Pol), and on the hybrid ED17 model via a genetic algorithm (GA - Hybrid), aluminium plate, (a) $a/h = 2.5$, (b) $a/h = 5$, (c) $a/h = 50$.

Figure 5. $\bar{\sigma}_{xx}$ distribution along the thickness of the aluminium plate, (a) $a/h = 2.5$, (b) $a/h = 5$.

Figure 6. BTDs based on ED4 models and built via the AAM (AAM − Pol), and on the hybrid ED17 model via a genetic algorithm (GA - Hybrid), bimetallic plate, (a) $a/h = 2.5$, (b) $a/h = 5$.

Figure 7. $\bar{\sigma}_{xx}$ distribution along the thickness of the bimetallic plate, (a) $a/h = 2.5$, (b) $a/h = 5$.

Tables

Table 1.

Expansion Order

1	2	3	4	5	6	7	8	9
1	z	z^2	z^3	z^4	$\sin\left(\frac{\pi z}{h}\right)$	$\sin\left(\frac{2\pi z}{h}\right)$	$\sin\left(\frac{3\pi z}{h}\right)$	$\sin\left(\frac{4\pi z}{h}\right)$
1	z	z^2	z^3	z^4	$\sin\left(\frac{\pi z}{h}\right)$	$\sin\left(\frac{2\pi z}{h}\right)$	$\sin\left(\frac{3\pi z}{h}\right)$	$\sin\left(\frac{4\pi z}{h}\right)$
1	z	z^2	z^3	z^4	$\sin\left(\frac{\pi z}{h}\right)$	$\sin\left(\frac{2\pi z}{h}\right)$	$\sin\left(\frac{3\pi z}{h}\right)$	$\sin\left(\frac{4\pi z}{h}\right)$

Expansion Order

10	11	12	13	14	15	16	17
$\cos\left(\frac{\pi z}{h}\right)$	$\cos\left(\frac{2\pi z}{h}\right)$	$\cos\left(\frac{3\pi z}{h}\right)$	$\cos\left(\frac{4\pi z}{h}\right)$	$e^{\frac{z}{h}}$	$e^{\frac{2z}{h}}$	$e^{\frac{3z}{h}}$	$e^{\frac{4z}{h}}$
$\cos\left(\frac{\pi z}{h}\right)$	$\cos\left(\frac{2\pi z}{h}\right)$	$\cos\left(\frac{3\pi z}{h}\right)$	$\cos\left(\frac{4\pi z}{h}\right)$	$e^{\frac{z}{h}}$	$e^{\frac{2z}{h}}$	$e^{\frac{3z}{h}}$	$e^{\frac{4z}{h}}$
$\cos\left(\frac{\pi z}{h}\right)$	$\cos\left(\frac{2\pi z}{h}\right)$	$\cos\left(\frac{3\pi z}{h}\right)$	$\cos\left(\frac{4\pi z}{h}\right)$	$e^{\frac{z}{h}}$	$e^{\frac{2z}{h}}$	$e^{\frac{3z}{h}}$	$e^{\frac{4z}{h}}$

Table 2.

Full model representation					Reduced model representation				
▲	▲	▲	▲	▲	▲	Δ	▲	▲	▲
▲	▲	▲	▲	▲	▲	▲	▲	▲	▲
▲	▲	▲	▲	▲	▲	▲	▲	▲	▲

Table 3.

Active term	Inactive terms
▲	Δ

Table 4.

a/h	100	10	5	2
3D	0.2037	0.2068	0.2168	0.3145
LD4	0.2037	0.2068	0.2168	0.3165

Table 5.

$$M_E = {}^4/_{51}$$

△	▲	△	△	△	△	△	△	△	△	△	△	△	△	△	△	△
△	△	△	▲	△	△	△	△	△	△	△	△	△	△	△	△	△
▲	△	△	△	△	△	△	△	△	△	△	△	△	△	△	△	▲

$$M_E = {}^5/_{51}$$

△	▲	△	△	△	△	△	△	△	△	△	△	△	△	△	△	△
△	△	△	▲	△	△	△	▲	△	△	△	△	△	△	△	△	△
▲	△	△	△	△	△	△	△	△	△	△	△	△	△	△	△	▲

$$M_E = {}^6/_{51}$$

△	▲	▲	△	△	△	△	△	△	△	△	△	△	△	△	△	△
△	△	△	▲	△	△	△	▲	△	△	△	△	△	△	△	△	△
▲	△	△	△	△	△	△	△	△	△	△	△	△	△	△	△	▲

$$M_E = {}^7/_{51}$$

△	▲	△	△	▲	△	△	△	△	▲	△	△	△	△	△	△	△
△	△	△	▲	△	△	△	△	△	△	△	△	△	△	△	△	△
▲	△	△	△	△	△	▲	△	△	△	△	△	△	▲	△	△	△

$$M_E = {}^8/_{51}$$

△	▲	△	△	▲	△	△	△	△	▲	△	△	△	△	△	△	△
▲	△	△	▲	△	△	△	△	△	△	△	△	△	△	△	△	△
▲	△	△	△	△	△	▲	△	△	△	△	△	△	▲	△	△	△

$$M_E = {}^9/_{51}$$

△	▲	△	△	△	△	△	△	△	▲	△	△	△	△	△	△	▲
△	▲	△	△	▲	△	△	△	△	△	△	△	△	△	△	▲	▲
▲	△	△	△	△	△	△	△	△	▲	△	△	△	△	△	△	△

Table 6.

M_E	% Error – Pol	% Error – Hybrid
$^4/_{51}$	5.3733	1.5256
$^5/_{51}$	3.0488	1.0681
$^6/_{51}$	2.2678	0.9818
$^7/_{51}$	1.8438	0.8775
$^8/_{51}$	1.4362	0.7697
$^9/_{51}$	1.2159	0.6849

Table 7.

$$M_E = \ ^5/_{51}$$

△	▲	△	△	△	△	△	△	△	△	△	△	△	△	▲	△
△	▲	△	△	△	△	△	△	△	△	△	△	△	△	△	△
▲	△	▲	△	△	△	△	△	△	△	△	△	△	△	△	△

$$M_E = \ ^6/_{51}$$

△	▲	△	△	△	△	△	△	△	△	△	△	△	△	▲	△
△	▲	△	△	△	△	▲	△	△	△	△	△	△	△	△	△
▲	△	▲	△	△	△	△	△	△	△	△	△	△	△	△	△

$$M_E = \ ^7/_{51}$$

△	▲	△	△	△	△	△	△	△	△	▲	△	△	△	▲	△	△
△	▲	△	△	△	△	▲	△	△	△	△	△	△	△	△	△	△
▲	△	▲	△	△	△	△	△	△	△	△	△	△	△	△	△	△

$$M_E = \ ^8/_{51}$$

△	▲	△	△	△	△	△	△	△	△	▲	△	△	△	▲	△	△
▲	▲	△	△	△	△	▲	△	△	△	△	△	△	△	△	△	△
▲	△	▲	△	△	△	△	△	△	△	△	△	△	△	△	△	△

$$M_E = \ ^9/_{51}$$

△	▲	△	△	△	△	△	△	△	△	▲	△	△	△	▲	△	△
▲	▲	△	△	△	△	▲	△	△	△	△	△	△	△	△	△	▲
▲	△	▲	△	△	△	△	△	△	△	△	△	△	△	△	△

Table 8.

M_E	% Error – Pol	% Error – Hybrid
$^5/_{51}$	1.5953	0.7624
$^6/_{51}$	0.9047	0.3665
$^7/_{51}$	0.5067	0.3143
$^8/_{51}$	0.4078	0.2956
$^9/_{51}$	0.3435	0.2782

Table 9.

$$M_E = {}^5/_{51}$$

Δ	▲	Δ	Δ	Δ	Δ	Δ	Δ	Δ	Δ	Δ	Δ	Δ	Δ	Δ	Δ	Δ
▲	Δ	Δ	Δ	Δ	Δ	Δ	Δ	Δ	Δ	Δ	Δ	Δ	▲	Δ	Δ	Δ
▲	Δ	Δ	Δ	Δ	Δ	Δ	Δ	Δ	▲	Δ	Δ	Δ	Δ	Δ	Δ	Δ

$$M_E = {}^6/_{51}$$

Δ	▲	Δ	Δ	Δ	Δ	Δ	Δ	Δ	Δ	Δ	Δ	Δ	Δ	Δ	Δ	Δ
▲	Δ	Δ	Δ	Δ	Δ	Δ	Δ	Δ	Δ	▲	Δ	Δ	▲	Δ	Δ	Δ
▲	Δ	Δ	Δ	Δ	Δ	Δ	Δ	Δ	▲	Δ	Δ	Δ	Δ	Δ	Δ	Δ

$$M_E = {}^7/_{51}$$

Δ	▲	Δ	Δ	Δ	Δ	Δ	▲	Δ	Δ	Δ	Δ	Δ	Δ	Δ	Δ	Δ
▲	Δ	Δ	Δ	Δ	Δ	Δ	Δ	Δ	Δ	▲	Δ	Δ	▲	Δ	Δ	Δ
▲	Δ	Δ	Δ	Δ	Δ	Δ	Δ	Δ	▲	Δ	Δ	Δ	Δ	Δ	Δ	Δ

$$M_E = {}^8/_{51}$$

Δ	▲	Δ	Δ	Δ	Δ	Δ	▲	Δ	Δ	Δ	Δ	Δ	Δ	Δ	Δ	Δ
▲	Δ	Δ	Δ	Δ	Δ	Δ	Δ	Δ	Δ	▲	Δ	▲	▲	Δ	Δ	Δ
▲	Δ	Δ	Δ	Δ	Δ	Δ	Δ	Δ	▲	Δ	Δ	Δ	Δ	Δ	Δ	Δ

Table 10.

M_E	% Error – Pol	% Error – Hybrid
$^5/_{51}$	2.6854	1.1179
$^6/_{51}$	2.0312	0.6227
$^7/_{51}$	1.8048	0.5467
$^8/_{51}$	1.6409	0.4550

Table 11.

$$M_E = {}^{5}/_{51}$$

▲	▲	Δ	Δ	Δ	Δ	Δ	Δ	Δ	Δ	Δ	Δ	Δ	Δ	Δ	Δ	Δ
Δ	Δ	Δ	▲	Δ	▲	Δ	Δ	Δ	Δ	Δ	Δ	Δ	Δ	Δ	Δ	Δ
▲	Δ	Δ	Δ	Δ	Δ	Δ	Δ	Δ	Δ	Δ	Δ	Δ	Δ	Δ	Δ	Δ

$$M_E = {}^{6}/_{51}$$

▲	▲	Δ	Δ	Δ	Δ	Δ	Δ	Δ	Δ	Δ	Δ	Δ	Δ	Δ	Δ	Δ
Δ	Δ	Δ	▲	Δ	▲	Δ	Δ	Δ	Δ	Δ	Δ	Δ	Δ	Δ	Δ	Δ
▲	▲	Δ	Δ	Δ	Δ	Δ	Δ	Δ	Δ	Δ	Δ	Δ	Δ	Δ	Δ	Δ

Table 12.

M_E	% Error – Pol	% Error – Hybrid
${}^{5}/_{51}$	2.9200	1.8927
${}^{6}/_{51}$	1.6858	1.5900

Figures

Figure 1.

Figure 2.

Displacement field

u_{x_1}	u_{x_2}	u_{x_3}	u_{x_4}	u_{x_5}
u_{y_1}	u_{y_2}	u_{y_3}	u_{y_4}	u_{y_5}
u_{z_1}	u_{z_2}	u_{z_3}	u_{z_4}	u_{z_5}

Genes of a chromosome

u_{x_1}	u_{x_2}	u_{x_3}	u_{x_4}	u_{x_5}	u_{y_1}	u_{y_2}	u_{y_3}	u_{y_4}	u_{y_5}	u_{z_1}	u_{z_2}	u_{z_3}	u_{z_4}	u_{z_5}

u_{x_4}, u_{y_3} and u_{z_3} activated

Δ	Δ	Δ	▲	Δ	Δ	Δ	▲	Δ	Δ	Δ	Δ	▲	Δ	Δ

Figure 3.

Figure 4.

(a) $a/h = 2.5$

(b) $a/h = 5$

(c) $a/h = 50$

Figure 5.

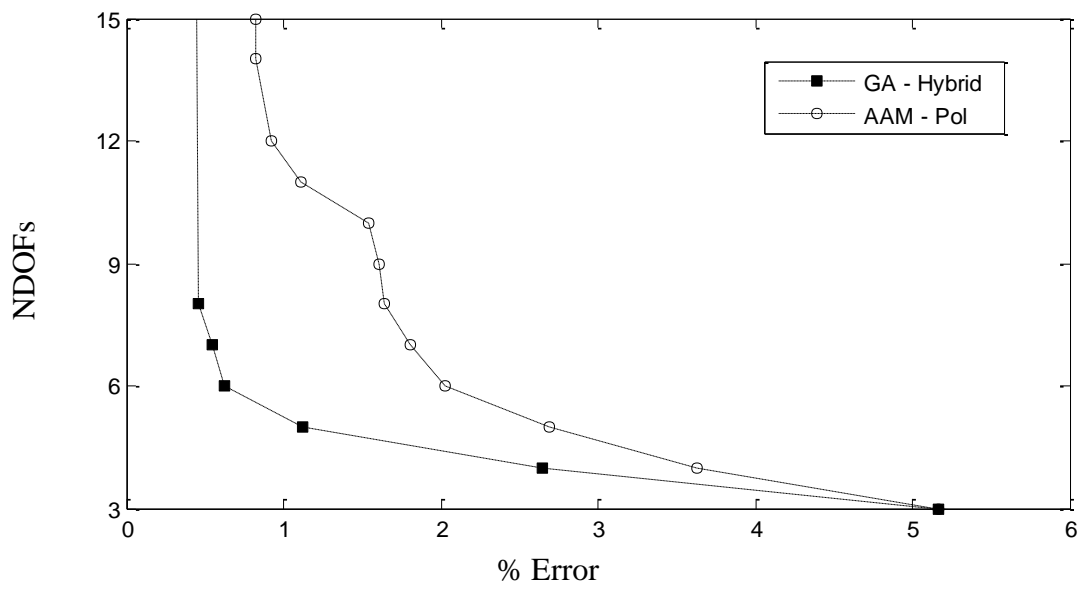(a) $a/h = 2.5$

(b) $\dfrac{a}{h} = 5$

Figure 6.

(a) $\dfrac{a}{h} = 2.5$

(b) $a/h = 5$

Figure 7.

(a) $a/h = 2.5$

(b) $a/h = 5$